Influence of Branch Content, Comonomer Type, and Crosshead Speed on the Mechanical Properties of Metallocene Linear Low-Density Polyethylenes

Ashraful Islam, Ibnelwaleed A. Hussein

Department of Chemical Engineering, King Fahd University of Petroleum & Minerals, Dhahran 31261, Saudi Arabia

Received 27 February 2005; accepted 12 September 2005
DOI 10.1002/app.23232
Published online in Wiley InterScience (www.interscience.wiley.com).

ABSTRACT: The effects of branch content (BC) and comonomer type on the mechanical properties of metallocene linear low-density polyethylene (m-LLDPEs) were studied by means of a stress–strain experiment at room temperature. A total of 16 samples with different BCs and comonomer types were used. In addition, the effect of crosshead speed on the mechanical properties of m-LLDPEs with different BCs was examined. The degree of crystallinity (X_t) of these copolymers was determined by differential scanning calorimetry. In addition, Ziegler–Natta linear low-density polyethylenes (ZN-LLDPEs) were also studied for comparison purposes. The increase in BC of m-LLDPEs decreased X_t and the modulus. However, the ZN-LLDPEs showed higher small-strain properties but lower ultimate properties than the m-LLDPEs with similar weight-average molecular weights and BCs. In comparison with low-BC resins, m-LLDPEs with high BCs exhibited a stronger strain hardening during the stress–strain experiments. Strain hardening was modeled by a modified Avrami equation, and the order of the mechanically induced crystal growth was in the range of 1–2, which suggested athermal nucleation. The crosshead speed was varied in the range 10–500 mm/min. For low-BC m-LLDPEs, there existed a narrow crosshead speed window within which the maxima in modulus and ultimate properties were observed. The location of the maxima were independent of BC. The effect of the crosshead speed on the mechanical properties of the m-LLDPEs was a strong function of BC. However, highly branched m-LLDPE in this experiment showed a weak dependence on the crosshead speed. J Appl Polym Sci 100: 5019–5033, 2006

Key words: mechanical properties; polyethylene (PE); branched; metallocene catalysts

INTRODUCTION

Metallocene-catalyzed polyethylenes have attracted great attention from film manufacturers since their commercial development. Metallocene linear low-density polyethylenes (m-LLDPEs) are now widely used in packaging film applications.[1] The major advantage of m-LLDPEs over conventional [Ziegler–Natta (ZN) type] LLDPEs is the possibility of the synthesis of ethylene copolymers with a narrow molecular weight distribution (MWD) and a homogeneous composition distribution. The lack of high- and low-molecular-weight tails in these copolymers have significant effects on their processing characteristics and physical properties.[2]

The microstructure of polymers plays an important role in the determination of their mechanical properties. A number of structural and morphological factors, such as type, concentration, and distribution of branching; degree of crystallinity (X_t); weight-average molecular weight (M_w); and MWD, directly influence the mechanical properties of polyethylenes.[3–10] Many researchers have investigated the effect of branch content (BC) and branch type on the crystallization behavior and mechanical properties of ethylene/α-olefin copolymers.[11–21] These authors have reported either the small-strain behavior or the properties of low-BC Ziegler–Natta linear low-density polyethylenes (ZN-LLDPEs).

Simanke et al.[11] studied the effect of branching on the mechanical properties of ethylene/1-hexene, 1-octene, 1-decene, 1-octadecene, and 4-methyl-1-pentene copolymers, and their results were limited to the small-strain behavior. They failed to obtain the full stress–strain curves of these copolymers due to slippage in the grips. The branch distribution and comonomer type at similar X_t values had only small effects on the modulus, but considerable variations were found in the modulus with increasing BC.[13,22] The initial modulus decreased monotonically with increasing branching, regardless of the crystallization mode.[22] Sehanobish et al.[13] also observed similar results and suggested that the modulus of the branched

Correspondence to: I. A. Hussein (ihussein@kfupm.edu.sa).
Contract grant sponsor: King Abdul Aziz City for Science and Technology; contract grant number: AT-22-16.
Contract grant sponsor: King Fahd University of Petroleum & Minerals.

polyethylene was primarily dominated by X_t. On detailed examination, Mandelkern and his coworkers[4,5] made clear that the effect of X_t on the modulus is complex.

Through an increase in the number of short-chain branches via the incorporation of α-olefin comonomers such as 1-butene, 1-hexene, and 1-octene, the polymer X_t and density can be reduced. These side chains do not crystallize and are rejected into the amorphous or interfacial regions.[11,12] m-LLDPEs are generally believed to have homogeneous composition distributions and narrow MWDs. So, m-LLDPEs provide an opportunity to investigate the roles of short-chain branching on the mechanical properties of these copolymers. So, the mechanical properties of LLDPEs are influenced by BC, comonomer type, and other molecular parameters, such as M_w and MWD. However, the previous work that studied the influence of BC and comonomer type on the mechanical properties was limited to small-strain properties. In this study, large-strain properties were obtained.

In addition, the mechanical properties of polymers can be influenced by the testing parameters. During mechanical testing, the effect of increasing deformation rate or crosshead speed on the low-strain portions of the stress–strain curve was suggested to be similar to the effect of increasing a sample's X_t or decreasing the test temperature.[2] Generally, for polymers, the *flow stress* (the stress needed for plastic flow) increases with temperature. The sensitive nature of flow stress on the crosshead speed and temperature can be described by Eyring's equation.[23] According to Eyring's equation, the slope of the linear dependence of yield stress on crosshead speed is related to a material's elemental motion unit and the testing temperature.

Understanding the effect of crosshead speed dependence on the deformation behavior of polyethylene is important for the ultimate users. The effect of crosshead speed on the deformation of polymers has received wide attention by many researchers.[24–30] In polyethylenes, until now no attention has been given to the influence of crosshead speed on polymers with different BCs. The crosshead speed has a strong effect on the deformation process of polymers because the energy used during plastic deformation is largely dissipated as heat. This effect was observed to be more prominent at high crosshead speeds associated with adiabatic drawing rather than during small crosshead speeds where isothermal drawing occurs.[26,28] Termonia et al.[29] reported that each molecular weight exhibits a different temperature or elongation window within which optimum drawing occurs. Within these windows, the rate of slippage of chains through entanglements reaches its optimum value. Again, the previous study did not examine the influence of BC on the crosshead speed dependency of the mechanical properties of m-LLDPEs.

In this work, metallocene copolymers of ethylene and 1-butene (m-EB), ethylene and 1-hexene (m-EH), and ethylene and 1-octene (m-EO) were used. The selected m-LLDPEs had similar M_w and MWD values. Our objective was to investigate the influence of BC and comonomer type on the mechanical properties of m-LLDPEs at small and large strains. For the first time, the effect of BC on the large-strain properties of m-LLDPEs was measured and modeled with a modified form of the Avrami equation. Some conventional LLDPEs (ZN-LLDPEs) were examined for comparison with m-LLDPEs of similar BCs, comonomer types, and M_w's. The influence of BC was studied with m-LLDPE with BCs in the range 14–42 branches/1000 C. To explore the consequences of varying the comonomer type, butene, hexene, and octene ethylene copolymers with selected BCs were used. In addition, the impact of crosshead speed on the mechanical properties of m-LLDPEs with different BCs was determined.

EXPERIMENTAL

Materials and sample preparation

Twelve commercial samples of m-LLDPEs, three ZN-LLDPEs, and one high-density polyethylene (HDPE) were used. The types of m-LLDPEs were as follows: four m-EBs, six m-EHs, and two m-EOs. The three ZN-LLDPEs, one from each comonomer type, were selected for comparison with the m-LLDPEs, and the linear HDPE was used as a reference. The HDPE represented a limiting case for the LLDPEs with low BCs because it had a zero BC. All samples were ExxonMobil products (Machelen, Belgium). M_w values of all LLDPEs (both metallocene and ZN) were close to 100 kg/mol, and the MWD of the m-LLDPEs was about 2. Hence, the only primary molecular variable was BC. Table I provides characterization data for all of the samples. Density and melt index (MI) values were provided by ExxonMobil. In addition, information about M_w and BC was determined by gel permeation chromatography and ^{13}C-NMR, respectively. Details about the gel permeation chromatography and the NMR characterizations were given in a previous publication.[31] The resins were named according to their branch type and BC. For example, a m-EB copolymer with a BC of 14.5 CH_3/1000 C was named m-EB15.

Mechanical testing

Compression molding was used to obtain sheets (~3 mm thick) in a Carver press (Wabash, IN) by the application of the following thermal history. At 170°C, a load of 1 metric ton (MT) was applied for 2 min, followed by a load of 3 MTs for 3 min, then a load of 5 MTs for 1 min, and a load of 7 MTs for 3 min; finally, the mold was water-cooled for 7 min. A pneumatic

TABLE I
Polymer Characterization

Resin	Density (g/cm^3)	MI (g/10 min)	M_w (kg/mol)	M_w/M_n	BC[a]
m-EB15	0.910	1.20	108	1.95	14.50
m-EB19	0.900	1.20	110	1.78	18.50
m-EB37	0.888	2.20	87	2.10	36.62
m-EB42	0.880	0.80	126	1.81	42.00
ZN-EB13	0.918	1.0	118	3.07	13.20
m-EH12	0.918	2.50	94	1.40	12.02
m-EH15	0.912	1.20	102	2.14	14.50
m-EH18	0.900	1.20	108	1.83	18.02
m-EH20	0.902	2.0	95	2.06	19.74
m-EH24	0.895	2.20	92	1.85	23.60
m-EH32	0.883	2.20	97	2.02	32.17
ZN-EH17	0.917	2.80	80	8.40	16.71
m-EO16	0.902	1.10	90	2.04	16.32
m-EO33	0.882	1.10	95	1.99	32.67
ZN-EO25	0.902	1.02	106	6.10	25.25
HDPE0	0.961	0.70	102	6.7	0.0

m_n, number-average molecular weight.
[a] CH_3/1000C.

punch cutter was used to cut dog-bone specimens from this plate according to ASTM D 638 (type V). The tensile tests were performed on an Instron 5567 tensile testing machine (Canton, MA) at room temperature (24°C). To prevent slippage between regular grips at higher strains, pneumatic side action grips were used. In a previous work, Simanke et al.[11] faced slippage problems; hence, large-strain mechanical properties were not obtained. All of the samples were tested at a crosshead speed of 125 mm/min with a gauge length of 25.40 mm. Also, m-EB15, m-EB42, and linear HDPE were tested at crosshead speeds of 10, 50, 125, 250, and 500 mm/min to examine the impact of crosshead speed on the mechanical properties. The results reported in this study are based on a minimum of five samples.

Differential scanning calorimetry (DSC)

DSC measurements were performed on a TA Q1000 instrument (New Castle, DE) under a nitrogen atmosphere. The nitrogen flow rate was 50 mL/min. The samples obtained from the Carver press were used to obtain X_t. Also, samples of PEs were collected from the fractured surface of the strained specimens. Samples of 5–10 mg were sliced and then compressed into nonhermetic aluminum pans. Then, heating from 0 to 150°C was carried out at a rate of 10°C/min. Calculations of X_t were based on a heat of fusion of 290 J/g for a polyethylene crystal.[32]

RESULTS AND DISCUSSION

Influence of BC

Figures 1–3 show the stress–strain behavior of butene, hexene, and octene m-LLDPEs with different BCs obtained at a crosshead speed of 125 mm/min. In general, the yield stress decreased with increasing BC. At large strains, the situation was quite different. Strain hardening was observed for almost all of the samples, and it was more pronounced in high-BC resins.

X_t

X_t values were obtained from DSC for all samples before and after the stress–strain experiments. The results are given in Table II. DSC testing of PE samples before the stress–strain experiment revealed the initial X_t, which influenced Young's modulus (E). On the other hand, the testing of the strained samples disclosed the influence of the strain-hardening behavior on the final X_t. The objective of testing strained samples was to check for induced crystallization due to the application of stress. Significant change in X_t (shown by underline) before and after the stress-strain

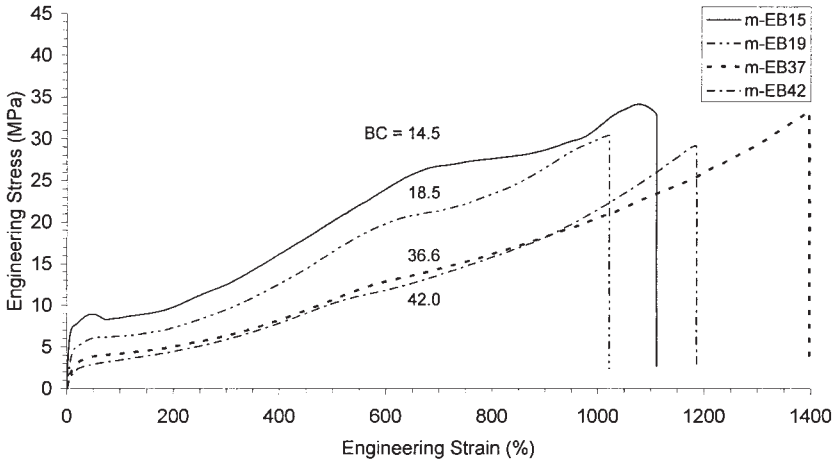

Figure 1 Stress–strain curves for m-EB m-LLDPEs with different BCs.

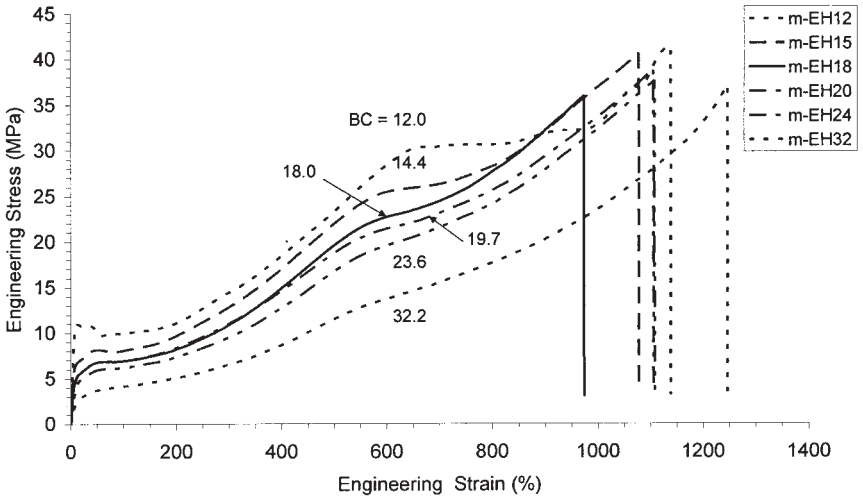

Figure 2 Stress–strain curves for m-EH m-LLDPEs with different BCs.

experiments was observed for the samples with high BC. The DSC thermograms of EB before and after mechanical testing are given in Figure 4. X_t changed slightly after deformation for copolymers with a high initial X_t (low BC). However, copolymers with BCs higher than 30 CH_3/1000 C exhibited an appreciable increase in their final X_t's after deformation (see Table II). Figure 4 shows a clear shift in the melting peak of the m-EB15 and m-EB19 resins.

Sumita et al.[33] showed that increases in both the heat of fusion and melting temperature (T_m) of polyethylene were due to the orientation of the amorphous phase as a result of drawing (induced crystallization). They proposed that the excess free energy of the amorphous phase resulting from orientation increased the T_m. This was a direct result of the decrease in change in entropy (ΔS) due to orientation; hence, change in Gibbs free energy (ΔG) was more positive ($\Delta G = \Delta H - T\Delta S$). The results in Table II show that samples with low BCs displayed an increase in T_m without any significant change in total X_t. So, it is likely that crystal perfection rather than induced crystallization took place. The low-BC m-LLDPEs had a high initial X_t. So, it was reasonable to assume that most of the applied stress was used to perfect the crystals. Crystal perfection due to the application of stress was previously observed for ZN-LLDPEs.[34] It was suggested that the more defective crystals of LLDPEs were destroyed during tensile testing and rebuilt into more perfect crystals.[34] This assumption was reinforced by our observation in this study that the strain hardening for low-BC resins was lower than that for high-BC m-LLDPEs.

The stress on samples with high BCs (more amorphous samples) resulted in an increased total X_t and a shift in T_m. However, for high-BC resins the peaks were very broad, and more than one melting peak was

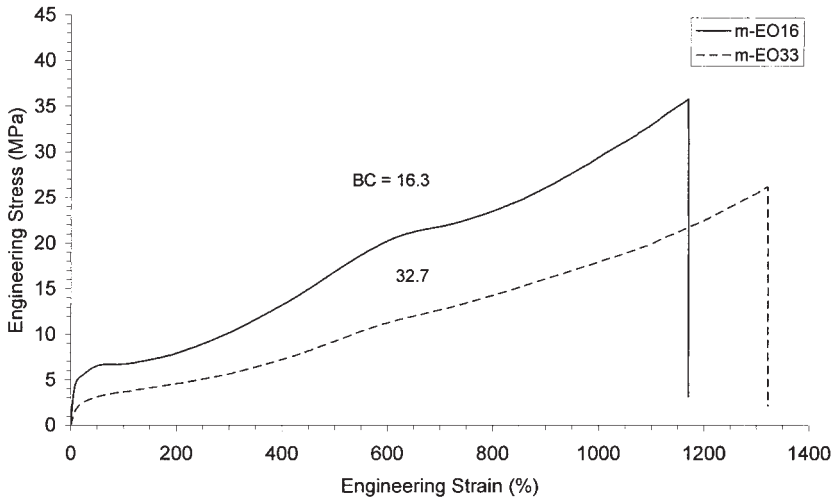

Figure 3 Stress–strain curves of for m-EO m-LLDPEs with different BCs.

TABLE II
Properties of the Ethylene/α-Olefins Copolymers

Resin	BC (CH_3/1000C)	Melting peak (°C)		DSC crystallinity value (%)	
		Before	After	Before	After
m-EB15	14.50	104.7	108.4	39.3	39.9
m-EB19	18.50	92.8	97.0	29.6	29.4
m-EB37	36.62	48.1, 71.0	43.2, 73.8	21.8	26.9
m-EB42	42.00	43.0, 63.2	46.4, 64.5	16.0	20.4
m-EH12	12.02	115.2	114.7	40.3	41.6
m-EH15	14.50	105.7	103.0	34.9	36.0
m-EH18	18.02	95.7	99.6	28.9	29.0
m-EH20	19.74	45.1, 88.3	45.4, 94.7	31.1	31.5
m-EH24	23.60	47.2, 90.3	43.2, 92.6	28.4	29.6
m-EH32	32.17	46.4, 73.2	44.7, 80.0	22.6	25.2
m-EO16	16.32	95.2	97.2	29.6	29.5
m-EO33	32.67	42.5, 72.2	44.9, 75.9	20.5	24.4

observed. Both melting peaks in m-EB37 and m-EB42 were shifted to higher temperatures. In addition, the applied stress improved the sharpness of the peak in high-BC resins. This suggested that part of the applied stress was used to perfect the weak crystals of highly branched m-LLDPEs and to increase the depth of the peaks (and increase X_t) as a result of induced crystallization. For high-X_t resins (m-EB15 and m-EB19), the shift in T_m was easy to detect.

Here, we would like to comment on the presence of two melting peaks in m-LLDPEs with high BCs. This was likely due to the poor branch distribution of m-LLDPE with high BCs, which led to linear portions and branched parts in the same molecule. Hence, crystallization of the different parts of the same molecule took place at different temperatures with branches being excluded from the crystalline lattice. Similar observations and explanations were given by Tanem and Stori[35] for copolymers with high BCs. The interfacial region may have had some ordering retained from the crystalline phase.[16] The DSC results show that strain-induced crystallization was more pronounced in the more amorphous resins (high-BC samples). So, it was likely that high stresses resulted in the perfection of crystals in low-BC samples and induced crystallization in high-BC resins.

The strain-induced crystallization resulted in an increase in stress with time. The increase in stress beyond the yield point was believed to be a result of orientation or induced crystallization. We marked the point at which the stress–time curve started to show an increase in stress as (σ_0, 0), where σ_0 is the stress at time zero. With time, the polymer X_t increased, and the stress needed to maintain a constant crosshead speed increased, too. This increase in stress continued until sample failure at (σ_f, t_f), where σ_f is the stress at sample failure and t_f is the time at sample failure. At any time on the stress–time curve (obtained from the stress–strain curve), the increase in stress ($\Delta\sigma = \sigma - \sigma_0$, where $\Delta\sigma$ is the change in stress and σ is the stress at a given time) induced the formation of crystals. In thermally induced crystallization, ΔT is the driving force for crystallization. On the other hand, $\Delta\sigma$ is the driving force for mechanically induced crystallization. Sumita et al.[33] obtained a linear relationship

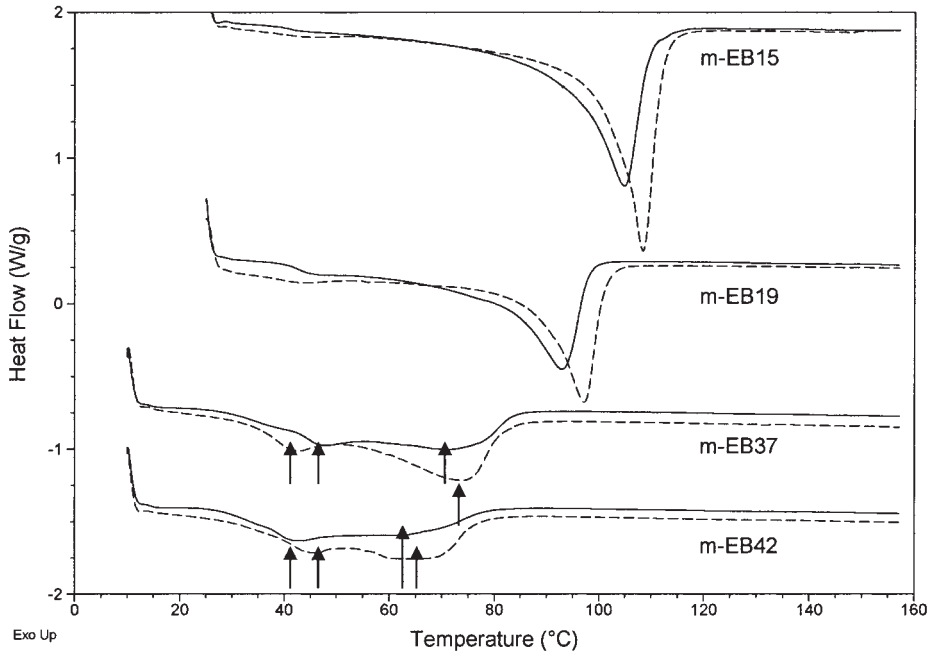

Figure 4 DSC thermograms of m-EBs (—) before and (- - -) after mechanical testing at a crosshead speed of 125 mm/min.

between the heat of fusion (proportional to X_t) and the melting point. Therefore, we were tempted to assume that the increase in stress was proportional to the increase in X_t ($\Delta\sigma \propto X_t$).

Hence, the fractional increase in stress $[(\sigma - \sigma_0)/(\sigma_f - \sigma_0)]$ was equal to the fractional increase in X_t. The physics of the mechanically and thermally induced crystallizations are similar. So, we were attracted to model the mechanically induced crystallization by a modified Avrami equation that is widely used in the study of the kinetics of crystallization.[36] We are not aware of any previous work that has attempted to use an Avrami-type equation to model mechanically induced crystallization. The well-known Avrami equation is defined as[37,38]

$$1 - X_t = \exp(-kt^n) \tag{1}$$

where n is the Avrami crystallization exponent dependent on the mechanism of nucleation, t is the time taken during the crystallization process, k is the growth rate constant, and X_t is the relative crystallinity of the polymers. Both k and n are constants that denote a given crystalline morphology and type of nucleation at particular crystallization conditions.[39] X_t is defined as follows:

$$X_t = \frac{\int_{t_0}^{t} (dH_c/dT)\, dT}{\int_{t_0}^{t_\infty} (dH_c/dT)\, dT} \tag{2}$$

where dH_c/dT is the rate of heat evolution and t_0 and t_∞ are the times at which crystallization starts and ends, respectively. Equation (1) was further modified by several authors to describe nonisothermal crystallization.[40–43] For nonisothermal crystallization at a chosen cooling rate (R), X_t is a function of the crystallization temperature (T). That is, eq. (2) can be rewritten as follows:

$$X_t = \frac{\int_{T_0}^{T} (dH_c/dT)\, dT}{\int_{T_0}^{T_\infty} (dH_c/dT)\, dT} \tag{3}$$

where T_0 and T_∞ represent the onset and final temperatures of crystallization, respectively.

t can be converted from temperature by the following equation.[40]

$$t = \frac{T_0 - T}{R} \tag{4}$$

where R is the cooling rate (°C/min). With eq. (1) in a double-logarithmic form

$$\ln[-\ln(1 - X_t)] = \ln k + n \ln t \tag{5}$$

and plotting $\ln[-\ln(1 - X_t)]$ versus $\ln t$ for each R, a straight line is obtained. From the slope and intercept of the lines, one can determine n and the crystallization rate constant (k). Here, the crystallization rate depends on R. Thus, k should be corrected adequately. At a constant R, k can be corrected as follows:[40]

$$\ln k' = \ln k/R \tag{6}$$

In this study, we have borrowed the idea of nonisothermal crystallization to model the crystallization induced by the applied stress during the stress–strain experiments. This method was applied only for ethylene–hexene samples due to the availability of a good number of samples of the same branch type. Therefore, X_t could be defined as follows:

$$X_t = \frac{\int_{\varepsilon_0}^{\varepsilon} (d\sigma_c/d\varepsilon)\, d\varepsilon}{\int_{\varepsilon_0}^{\varepsilon_f} (d\sigma_c/d\varepsilon)\, d\varepsilon} \tag{7}$$

where ε_0 and ε_f are the onset and final points of engineering strain (mm/mm) in the stress–strain curve where an increase in stress is observed due to strain hardening. ε is the strain at any time t. For all ethylene–hexene samples, ε_0 was taken at 150%. ε_f was taken 15 s before the sample failure, except for m-EH12. For m-EH12, ε_f was taken up to 650% because beyond this point, the stress–time curve was flat. t was converted from the engineering strain by the following equation:

$$t = \frac{\varepsilon_0 - \varepsilon}{D} \tag{8}$$

where D is the strain rate (min^{-1}). D was calculated in the following way:

$$\text{Strain rate} = \frac{\text{Crosshead speed(mm/min)}}{\text{Initial specimen length(mm)}} = \frac{125\text{(mm/min)}}{25.4\text{(mm)}} = 4.92\ (\text{min}^{-1})$$

At a constant D, k can be corrected as follows:

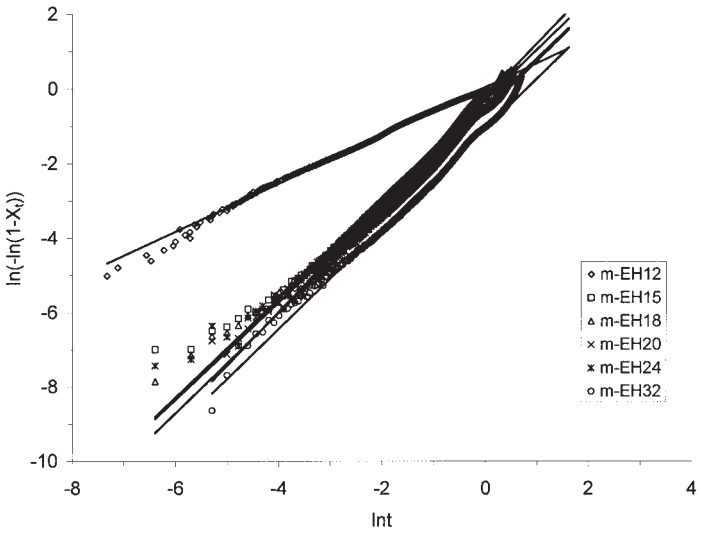

Figure 5 Avrami plot for m-EH m-LLDPEs ($D = 4.92\ \text{min}^{-1}$).

$$\ln k' = \ln k/D \tag{9}$$

Figure 5 shows a plot of $\ln[-\ln(1 - X_t)]$ versus $\ln t$ for m-EH m-LLDPEs resins. The Avrami parameters estimated from Figure 5 are listed in Table III. n was in the range 1–2, which suggested athermal nucleation (see p 147, ref. 39). However, for low-BC samples (m-EH12), n was less than 1, which suggested a different nucleation mode. This finding should be confirmed by other techniques, which was beyond the scope of this study.

E and yield stress

Figure 6 shows an expanded view of the stress–strain curves in the vicinity of yielding. The yield peak became less distinct with increasing BC regardless of the comonomer type. Also, the yielding region broadened with an increase in BC. Similar observations were reported by Bensason et al.[14] A double-yield phenomenon was also observed for samples with BCs less than 20. At the first yield point, temporary plastic deformation was assumed, followed by a recoverable recrystallization of the lamellae. The second point was the onset of permanent plastic deformation in which the lamellae were destroyed.[44] It was postulated that the double-yielding phenomena was due to a partial melting recrystallization process. With deformation, the melted species recrystallize in the draw direction with a simultaneous reduction in stress.[45,46]

TABLE III
Avrami Parameters for m-EH *m*-LLDPEs

Resin	n	k'
m-EH12	0.65	1.010666
m-EH15	1.34	0.948392
m-EH18	1.31	0.909502
m-EH20	1.44	0.959755
m-EH24	1.35	0.889249
m-EH32	1.34	0.808478

In general, copolymers with lower α-olefin contents showed higher yield stresses and E values. Our results suggest that the yield stress did not depend on the branch type but rather on BC. This result agreed with the observations of Simanke et al.[11] The results of E as a function of BC for all m-LLDPEs are presented in Figure 7. The error bars indicate the range of these results for a minimum of five samples. In Figure 7, a relationship (modulus = $15{,}279\text{BC}^{-1.748}$) is introduced to fit all of the data points. It is clear from Figure 7 that the modulus decreased with increasing BC, but the relationship was not linear. For linear PE (HDPE), the modulus was about 1100 MPa, whereas the m-LLDPEs showed a modulus in the range of 30–240 MPa depending on BC. The influence of X_t on the modulus was suggested to be complex.[4] The modulus is not a linear function of X_t. Researchers have tried to describe the plot by an S-shaped curve. Branched polymers with E in the range of 100–200 MPa fall in the lower part of the S shaped curve, which agrees very well with these results. A comparison between the m-LLDPEs and ZN-LLDPEs revealed that the ZN-LLDPEs possessed higher moduli than the m-LLDPEs of the same branch type and with similar average BCs. It was likely that the presence of linear molecules as a result of the structural and size heterogeneity of ZN-LLDPE were behind this observation.[20,47] As indicated by our results for the linear HDPE, the linear molecules showed a higher modulus. So, branch or composition distribution was another factor that influenced the mechanical properties of the LLDPEs.

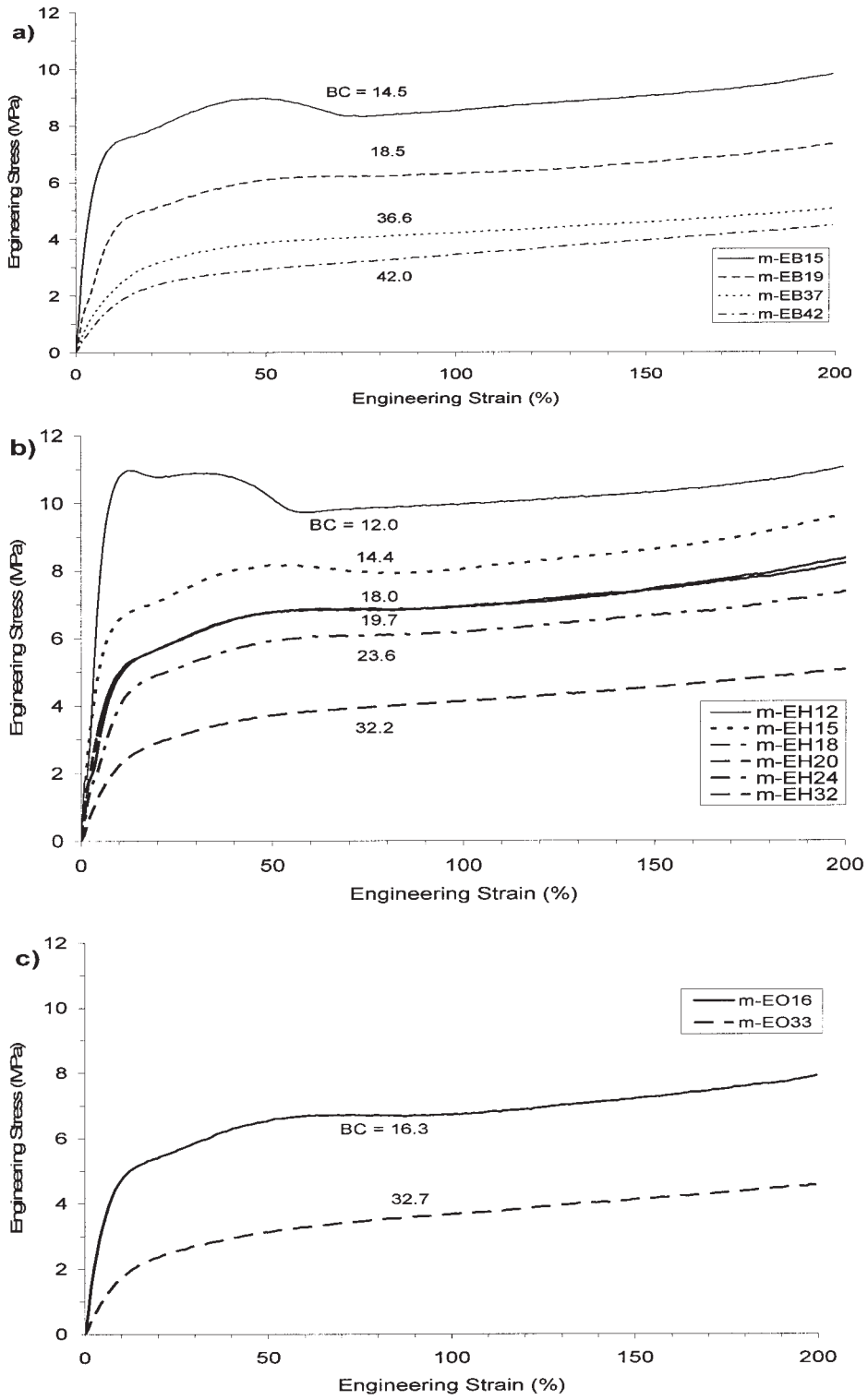

Figure 6 Yield phenomena at a crosshead speed of 125 mm/min.

Ultimate properties

The major ultimate properties we discuss are elongation at break (%) and ultimate tensile strength. In addition, another property, called *ultimate modulus* (UM), was introduced to measure the degree of strain hardening. It is the slope of the stress–strain curve near the ultimate values. Figure 8 shows the estimated UM as a function of BC. It is clear from Figure 8 that the relationship between UM and BC was complex. In general, EB and EH resins showed similar strain-hardening behaviors. For most of the samples, UM was in the range 3–11 MPa, whereas *E*

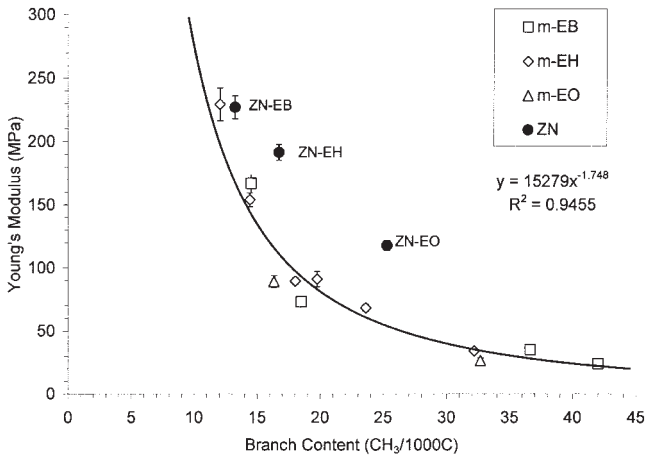

Figure 7 E as a function of BC (crosshead speed = 125 mm/min).

(the initial slope of the stress–strain curve) was in the range 30–240 MPa. ZN-LLDPEs showed less strain hardening than m-LLDPEs, which was a direct consequence of the composition distribution.

The elongation at break (%) as a function of BC is shown in Figure 9. Our results for the m-LLDPEs suggested that the elongation at break (%) was not a strong function of BC or comonomer type. These results agreed with previous observations reported on ZN-LLDPEs.[4,34] The ultimate properties were reported to be independent of the morphological and structural variables and did not depend on the M_w, MWD, or comonomer concentration as suggested by work on low-BC ZN-LLDPEs.[4]

The influence of BC on the ultimate tensile strength is shown in Figure 10. For ethylene–butene copolymers, BC showed no influence on ultimate tensile strength. For ethylene–hexene and ethylene–octene resins, the ultimate tensile strength showed a weak dependency on BC. In general, BC had a weak effect on the ultimate tensile strength. These results on the effect of BC of m-LLDPEs on ultimate properties were in agreement with previous observations on ZN-LLDPEs.[4] For the influence of comonomer type, ultimate tensile strength decreased slightly with increasing BC for ethylene–hexene resins. Also, m-EH resins exhibited higher stresses at break compared to m-EBs. As shown in Figures 9 and 10, ZN-LLDPEs displayed lower elongation at break and tensile strength values compared to m-LLDPEs. So, comonomer type and content of m-LLDPEs had weak effects on the ultimate tensile strength and strain at break. However, a complex relationship existed with UM (strain-hardening behavior).

Effect of crosshead speed

In general, higher crosshead speeds are suggested to give rise to increased elastic modulus, higher yield stress, and lower elongation at break values and a more defined neck.[2,48] Figure 11 shows E as a function of crosshead speed for three resins with different BCs. Figure 11(a–c) correspond to PEs with BCs of 0 (linear HDPE), 15 (m-EB15) and 42 (m-EB42), respectively. An interesting phenomenon was observed. For all three resins, it seemed that there existed a critical value (in the range 50–125 mm/min) after which E was not affected much by the crosshead speed. The location of the maximum was independent of BC. For HDPE, E, yield stress, and other parameters associated with the strain response were reported to decrease rapidly with increasing crosshead speed, when the crosshead speed was larger than a critical value.[25] Liu and Harrison[25] reported this critical value for polyethylene near a crosshead speed 100 mm/min (see Fig. 14, ref. 25), which was in agreement with our observations. The normal time–temperature superposition principle did not appear to hold in this case. The authors suggested that this decrease in modulus and yield stress was not caused by a temperature rise during strain. However, it may have been caused by void formation and crazing, which was relatively uniform throughout the sample. They provided an optical microscopic picture of polypropylene (see Fig. 7, ref. 25) to support their assumption.

The elongation at break and ultimate tensile strength as a function of crosshead speed for m-LLDPEs with different BCs are shown in Figures 12 and 13, respectively. The percentage elongation at break of linear HDPE decreased immediately with increasing crosshead speed as shown in Figure 12. The ultimate tensile strength of HDPE was not included, as it was broken immediately after it reached its yield point. Again, a critical value was observed, as shown in Figures 12 and 13(a), for m-EB15 at a crosshead speed of 125 mm/min. Termonia et al.[29] reported that for each M_w of melt-crystallized monodispersed PE, there existed a very narrow temperature or elongation rate window within which maximum drawability occurred. Although it was true for m-EB15, it did not hold for m-EB42. Also, increasing the speed from 125 to 250 mm/min did not affect the ultimate tensile strength. These results show that the elongation at break and tensile strength for m-EB42 were almost independent of crosshead speed [Figs. 12 and 13(b)] over a wide range. However, at very high crosshead speeds (500 mm/min), the ultimate properties dropped very fast. This may have been due to the high amorphous portion in m-EB42, which enhanced the possibility of void formation and crazing.[25]

An examination of Figures 11–13 for the combined influence of crosshead speed and BC on the mechanical properties showed some interesting observations.

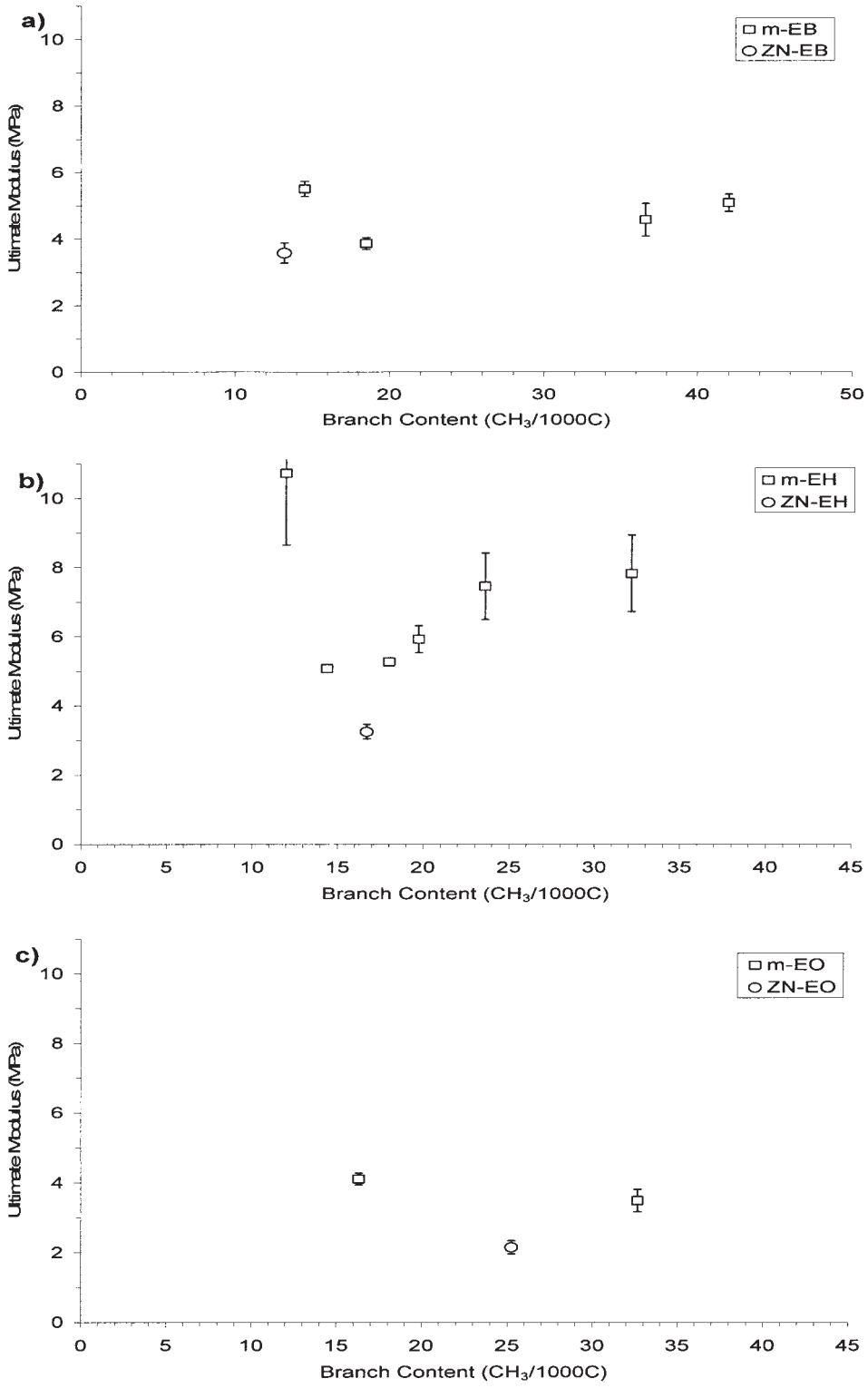

Figure 8 UM as a function of BC (crosshead speed = 125 mm/min).

We compare the properties obtained at a very low speed (10 mm/min) with that measured at very high (500 mm/min) speeds. The modulus of linear HDPE showed a decrease of about 30%. However, the modulus of branched m-LLDPEs at 500 mm/min retained almost the same values as those obtained at 10 mm/min. Hence, the crosshead speed had no or little effect on the modulus of the m-LLDPEs regardless of their BC. However, it influenced the modulus of linear HDPE. It was likely that the high strains led to the

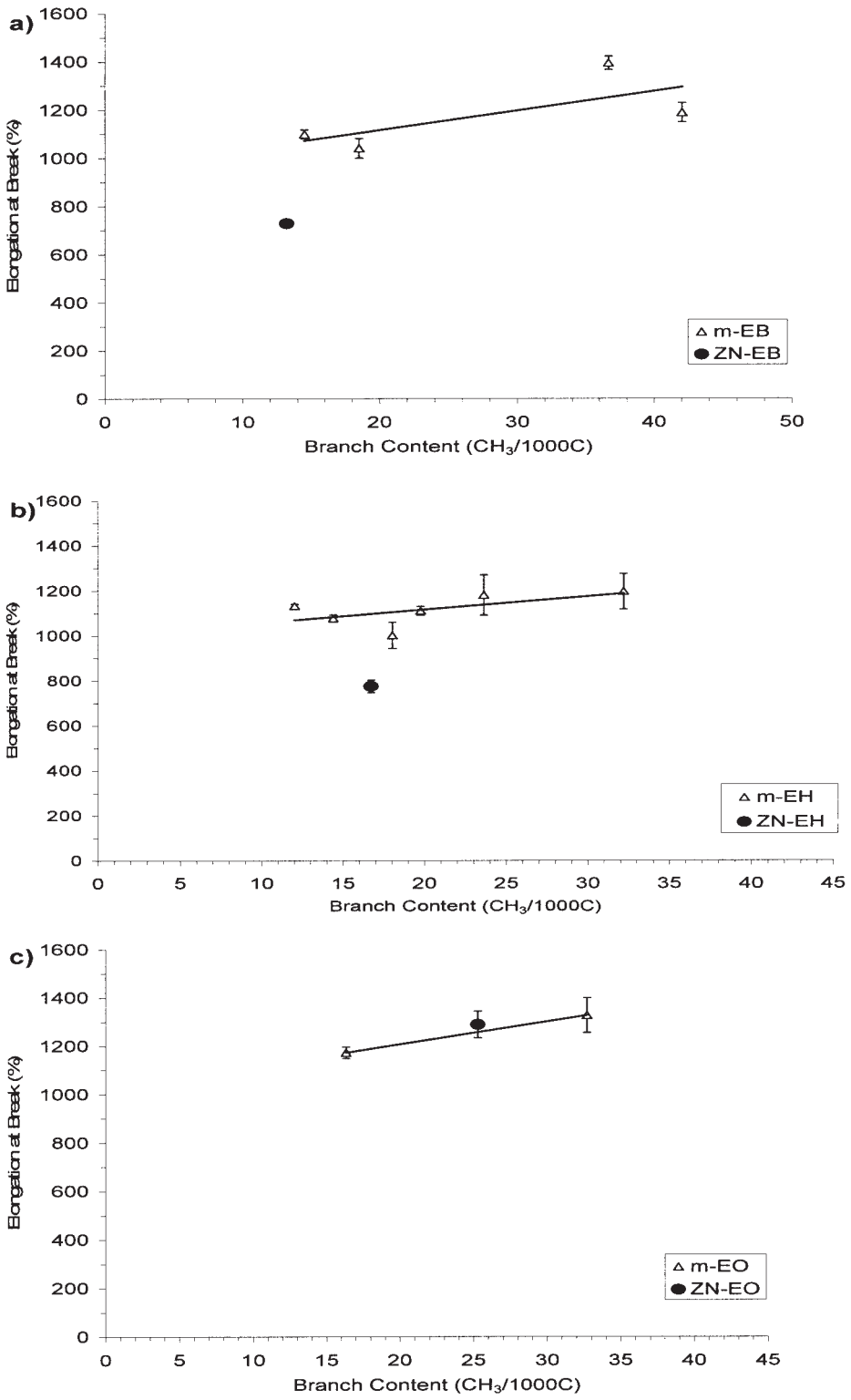

Figure 9 Elongation at break as function of BC (crosshead speed = 125 mm/min).

immediate destruction of crystals. For large-strain properties, such as elongation at break, the influence of crosshead speed was BC-dependent. The linear HDPE suffered the highest difference (>500 times) between the low and high rates due to its high X_t. On the other hand, the elongation at break of m-EB15 was reduced by about 50%, and that of the highly branched m-EB42 was lowered by about 15%. This was likely a result of the rubbery nature of the highly branched (more amorphous) m-LLDPEs. The elonga-

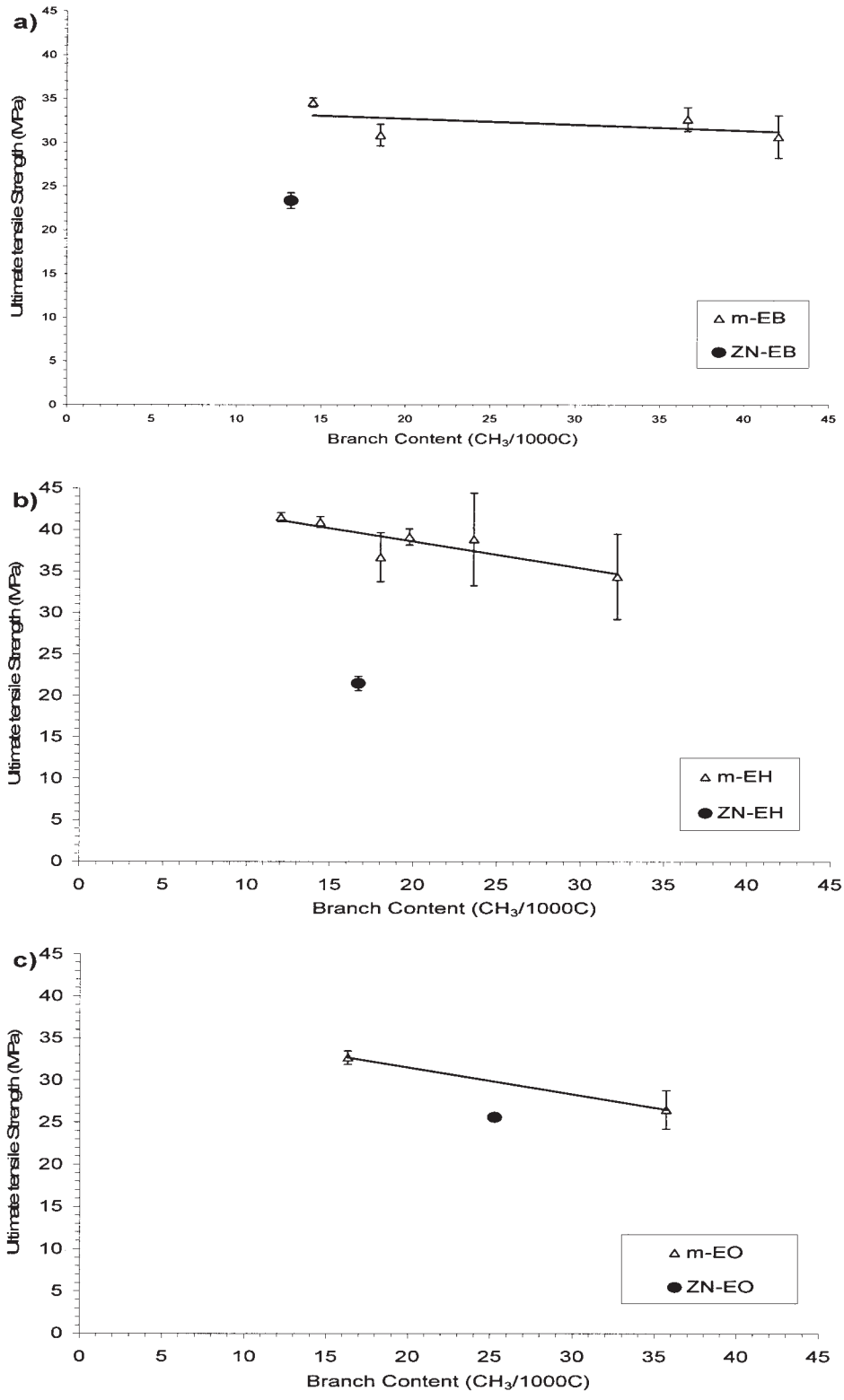

Figure 10 Ultimate tensile strength as function of BC (crosshead speed = 125 mm/min).

tion at break at high crosshead speeds (with a short process time and more solid-like behavior) was lower than that obtained at low crosshead speeds (with a long process time and liquid-like behavior). The overall behavior could be explained by a Deborah number effect. Also, the previous results show that branch type had no influence on E, yield stress, or the ultimate properties of the m-LLDPEs.

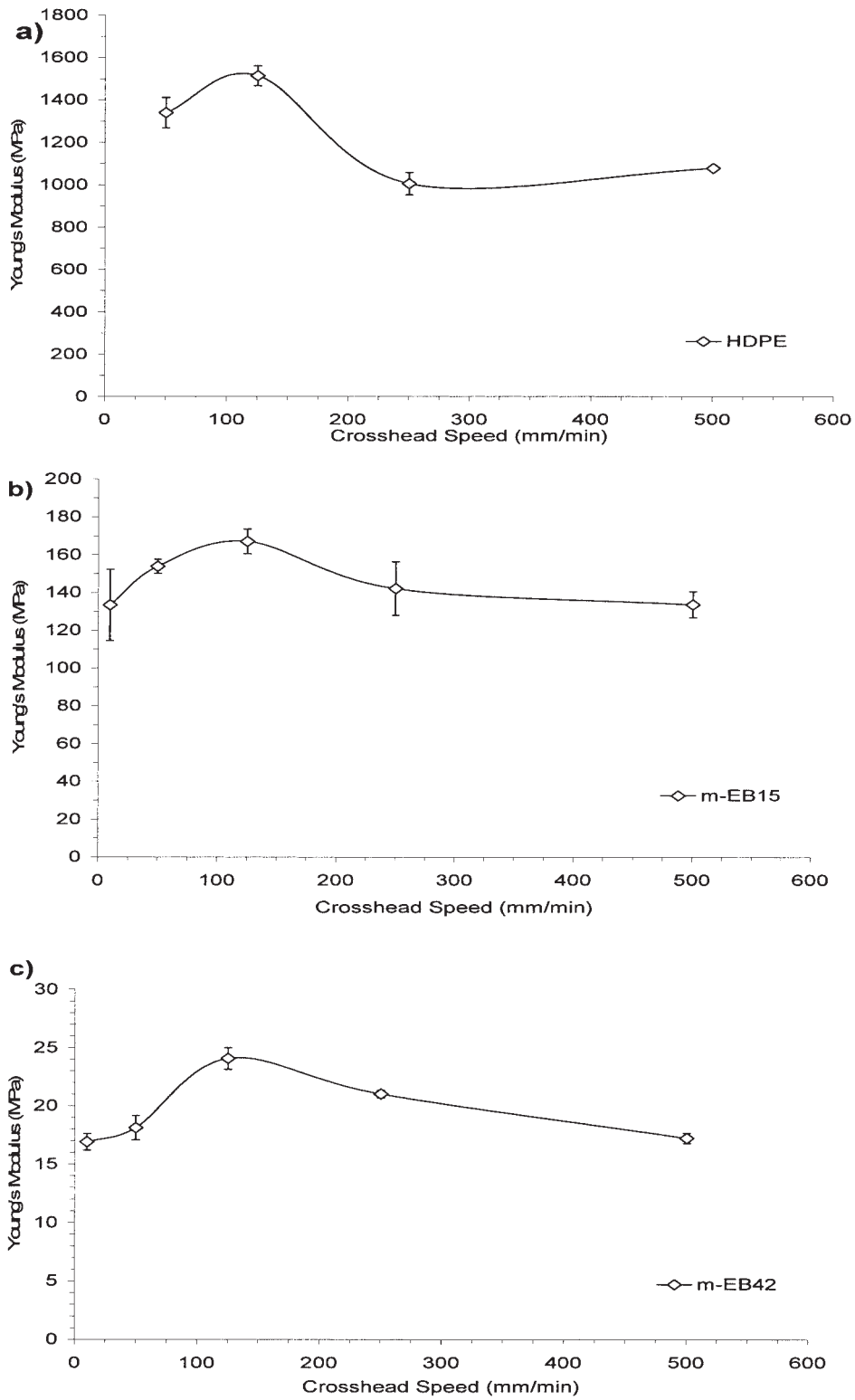

Figure 11 E as function of crosshead speed and BC.

CONCLUSIONS

The following conclusions can be drawn from the previous discussion:

1. Samples with low BCs displayed an increase in T_m without any significant change in total X_t. An increase in T_m and a significant increase in total X_t was observed for the high-BC samples. For the

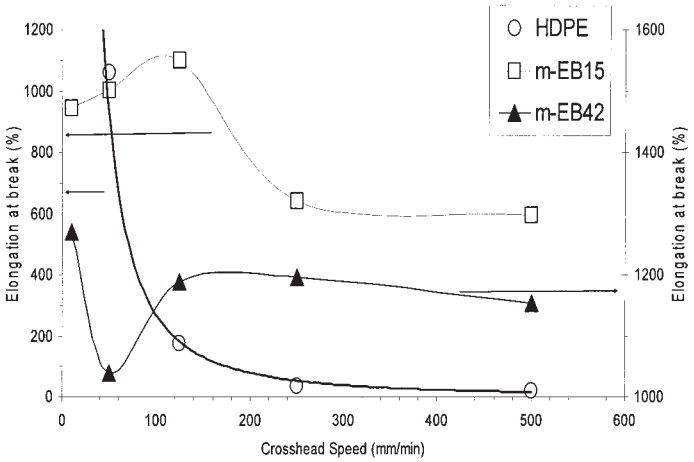

Figure 12 Elongation at break (%) as a function of crosshead speed and BC.

high-BC samples, the peaks were broad, and multiple melting peaks were observed.

2. E was directly influenced by BC, and a power series relationship ($E = 15{,}279\mathrm{BC}^{-1.748}$) was obtained. E was independent of branch type. ZN-LLDPEs showed higher values compared to m-LLDPEs because of the contribution of the linear components.
3. The yield stress became less distinct and broader with increasing BC regardless of comonomer type.
4. The ultimate properties of m-LLDPEs showed a weak dependency on BC and comonomer type.
5. ZN-LLDPEs showed higher small-strain properties (modulus and yield stress) but lower large-strain properties (elongation at break, ultimate tensile strength, and UM) than m-LLDPEs of similar M_w and BC.
6. An interesting phenomenon was observed because of the influence of crosshead speed. There existed a critical value (near a crosshead speed of 125 mm/min) after which E was not much influenced by the crosshead speed. The position of the maximum was independent of BC.
7. The elongation at break of linear HDPE decreased immediately with increasing crosshead speed.
8. For low-BC m-LLDPE, a maximum value was observed both for elongation at break and ultimate tensile strength at a crosshead speed of 125 mm/min. However, a minimum in elongation at break was obtained for high-BC m-LLDPE at a crosshead speed of 50 mm/min. At low crosshead speeds (<125 mm/min), a wide range of ultimate tensile strength behavior was observed for high-BC m-LLDPEs a function of the crosshead speed. However, at higher crosshead speeds, the ultimate tensile strength of high-BC m-LLDPEs dropped very fast.
9. A modified Avrami equation could describe and fit very well the strain-induced crystallization. The kinetics of the mechanically induced crystal-

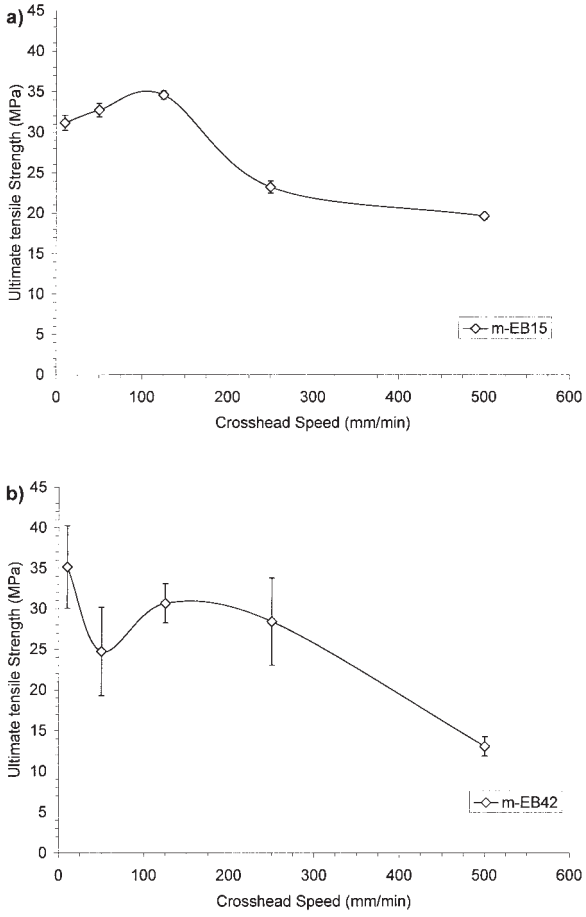

Figure 13 Tensile strength (MPa) as function of crosshead speed and BC.

lization could be fitted by an order of 1–2, which suggested athermal nucleation.

References

1. Miller, B. G.; Nally, G. M.; Murphy, W. R. ANTEC 2002, 2415.
2. Peacock, A. J. Handbook of Polyethylene: Structures, Properties, and Applications; Marcel Dekker: New York, 2000; p 516.
3. Mandelkern, L. Polym J 1985, 17, 337.
4. Popli, R.; Mandelkern, L. J Polym Sci Part B: Polym Phys 1987, 25, 441.
5. Kennedy, M. A.; Peacock, A. J.; Mandelkern, L. Macromolecules 1994, 27, 5297.
6. Kontou, E.; Niaounakis, M.; Spathis, G. Eur Polym J 2002, 38, 2477.
7. Graham, J. T.; Alamo, R. G.; Mandelkern, L. J Polym Sci Part B: Polym Phys 1997, 35, 213.
8. Sacristan, J.; Benavente, R.; Perena, J. M.; Perez, E.; Bello, A.; Rojas, R.; Quijada, R.; Rabagliati, F. M. J Therm Anal Calorim 1999, 58, 559.
9. Jordens, K.; Wilkes, G. L.; Janzen, J.; Rohlfing, D. C.; Welch, M. B. Polymer 2000, 41, 7175.
10. Li Pi Shan, C.; Soares, J. B. P.; Pendelis, A. Polymer 2002, 43, 767.
11. Simanke, A. G.; Galland, G. B.; Baumhardt, N. R.; Quijada, R.; Mauler, R. S. J Appl Polym Sci 1999, 74, 1194.
12. Kale, L.; Plumley, T.; Patel, R.; Redwine, O.; Jain, P. J Plast Film Sheeting 1995, 12, 27.
13. Sehanobish, K.; Patel, R. M.; Croft, B. A.; Chum, S. P.; Kao, C. I. J Appl Polym Sci 1994, 51, 887.
14. Bensason, S.; Minick, J.; Moet, A.; Chum, S.; Hiltner, A.; Baer, E. J Polym Sci Part B: Polym Phys 1996, 34, 1301.
15. Alamo, R. G.; Viers, B. D.; Mandelkern, L. Macromolecules 1993, 26, 5740.
16. Alamo, R.; Domszy, R.; Mandelkern, L. J Phys Chem 1984, 88, 6587.
17. Minick, J.; Moel, A.; Hiltner, A.; Baer, E.; Chum, S. P. J Appl Polym Sci 1995, 58, 1371.
18. Seguela, R.; Rietsch, F. Polymer 1986, 27, 703.
19. Xu, X.; Xu, J.; Feng, L.; Chen, W. J Appl Polym Sci 2000, 77, 1709.
20. Hussein, I. A. Polym Int 2004, 53, 1327.
21. Hussein, I. A.; Hameed, T. Macromol Mater Eng 2004, 289, 198.
22. Peacock, A. J.; Mandelkern, L. J Polym Sci Part B: Polym Phys 1990, 28, 1917.
23. Ward, I. M.; Hadley, D. W. An Introduction to the Mechanical Properties of Solid Polymers, 3rd ed.; Wiley: New York, 2000; p 237.
24. Andrew, J. M.; Ward, I. M. J Mater Sci 1970, 5, 411.
25. Liu, T.; Harrison, I. R. Polymer 1988, 29, 233.
26. Dasari, A.; Duncan, S. J.; Misra, R. D. K. Mater Sci Tech 2002, 18, 1227.
27. Dasari, A.; Misra, R. D. K. Mater Sci Eng A 2003, 358, 356.
28. Van der Wal, A.; Mulder, J. J.; Gaymans, R. J. Polymer 1998, 39, 5477.
29. Termonia, Y.; Allen, S. R.; Smith, P. Macromolecules 1988, 21, 3485.
30. Brooks, N. W.; Unwin, A. P.; Duckett, R. A.; Ward, I. M. J Polym Sci Part B: Polym Phys 1997, 35, 545.
31. Hameed, T.; Hussein, I. A. Polymer 2002, 43, 6911.
32. Mark, H. F.; Bikales, N. M.; Overberger, C. G.; Menges, G. Encyclopedia of Polymer Science and Engineering, 2nd ed.; Wiley: New York, 1986; Vol. 6, p 477.
33. Sumita, M.; Miyasaka, K.; Ishikawa, K. J Polym Sci Part B: Polym Phys 1977, 15, 837.
34. Seguela, R.; Rietsch, F. Polymer 1986, 27, 532.
35. Tanem, B. S.; Stori, A. Polymer 2001, 42, 5389.
36. Wunderlich, B. In Thermal Characterization of Polymeric Materials; Turi, E. A., Ed.; Academic: New York, 1997; Vol. 1, p 252.
37. Avrami, M. J Chem Phys 1939, 7, 1103.
38. Avrami, M. J Chem Phys 1940, 8, 212.
39. Wunderlich, B. Macromolecular Physics; Academic: New York, 1976; Vol. 2, p 147.
40. Jeziorny, A. Polymer 1978, 19, 1142.
41. Tobin, M. C. J Polym Sci Part B: Polym Phys 1974, 12, 399.
42. Juana, R. D.; Jauregui, A.; Calahora, E.; Cortazar, M. Polymer 1996, 37, 3339.
43. Herrero, C. H.; Acosta, J. L. Polym J 1994, 26, 786.
44. Brooks, N. W. J.; Duckett, R. A.; Ward, I. M. Polymer 1999, 40, 7367.
45. Flory, P. J.; Yoon, D. Y. Nature 1978, 272, 226.
46. Lucas, J. C.; Failla, M. D.; Smith, F. L.; Mandelkern, L. Polym Eng Sci 1995, 35, 1117.
47. Usami, T.; Gotoh, Y.; Takayama, S. Macromolecules 1986, 19, 2722.
48. Freid, J. R. Polymer Science and Technology; Prentice Hall: Upper Saddle River, NJ, 2003; Vol. 2.